Preparation and Sorption Studies of Microsphere Copolymers Containing β-Cyclodextrin and Poly(acrylic acid)

Rui Guo, Lee D. Wilson

Department of Chemistry, University of Saskatchewan, Saskatoon, Saskatchewan, S7N 5C9

Received 15 May 2011; accepted 1 October 2011
DOI 10.1002/app.36272
Published online 17 January 2012 in Wiley Online Library (wileyonlinelibrary.com).

ABSTRACT: Microsphere polymeric materials containing β-cyclodextrin (β-CD) and poly(acrylic acid) (PAA) with tunable morphologies were prepared in order to improve their sorption characteristics in aqueous solution. The microsphere polymeric materials were prepared using a (water/oil) micro-emulsion-evaporation technique to condense β-cyclodextrin (β-CD) with PAA at various comonomer ratios and mixing speeds. The β-CD microsphere copolymers were characterized using FTIR, TGA, DSC, SEM, elemental (C and H) microanalyses, and solid state ^{13}C-NMR spectroscopy. The sorption properties of the polymeric materials at 295 K in aqueous solution containing *p*-nitrophenol (PNP) were studied using a dye-based method with UV–Vis spectrophotometry at pH 4.6 and 10.3. The sorption isotherms of copolymer/PNP systems were evaluated with various isotherm models (e.g., Langmuir, BET, Freundlich, and Sips). The Sips isotherm showed the best overall agreement with the experimental results and the sorption parameters provided estimates of the sorbent surface area (12.0–331 m^2/g) and the sorption capacity (Q_m = 0.359–2.20 mmol/g at pH = 4.6; Q_m = 0.070–0.191 mmol/g at pH = 10.3) for the microsphere copolymer/PNP systems in aqueous solution. The nitrogen adsorption properties of the microporous copolymers in the solid state were obtained at 77K with BET surface areas ranging from 0.275 to 4.47 m^2/g. © 2012 Wiley Periodicals, Inc. J Appl Polym Sci 125: 1841–1854, 2012

Key words: cyclodextrin; poly(acrylic acid); copolymers; sorbents; grafting; sorption properties; *p*-nitrophenol

INTRODUCTION

Phenolic compounds are widely used as raw materials in the chemical industry[1] and other applications including petrochemical processing, kraft pulp and paper production, and olive oil products.[1,2] Phenolic compounds are found extensively in effluent streams and are considered as primary pollutants in waste water due to their relatively high toxicity, high biochemical oxygen demand, and relatively low biodegradability.[3] The accumulation and transport of phenol-based pollutants are important environmental issues, which adversely impact aquatic ecosystems, biodiversity, and human health.[1,3,4] The United Nations Environment Program (UNEP) has recognized the importance of safe and clean drinking water by making it one of the eight millennium goals to reduce the proportion of people without sustainable access by half in 2015.[4] Therefore, there is an urgent need to develop novel materials and innovative methods to address the removal of water borne phenols in contaminated aquatic environments.

Cyclodextrins (CDs) are water soluble cyclic oligosaccharides composed of six, seven, or eight glucopyranose units linked by α-1,4-glycosidic bonds; hereafter, they are referred to as α-, β-, and γ-cyclodextrin. CDs possess a torus-shaped macrocyclic structure with a hydrophilic exterior and a lipophilic interior [*cf*. Fig. 1(A)]. The lipophilic cavity of the various CDs are suitably sized for the inclusion of low to medium sized lipophilic molecules[5]; with a depth of 7.8 Å and inner macrocyclic diameters of 5.7 Å (α-CD), 7.8 Å (β-CD), and 9.5 Å (γ-CD). CDs were recently used as pore templates to form microporous and nanoporous materials because of their well-defined structure, relatively low toxicity, versatility, and the ability to form inclusion complexes.[6] CDs can be used to construct copolymer frameworks by chemical cross-linking, grafting or noncovalent self-assembly.[6,7] In this study, β-CD was used because it forms stable inclusion complexes with a wide range of inorganic and organic guest compounds. In the case of the latter, compounds containing benzyl and naphthyl moieties are known to form thermodynamically stable inclusion complexes in aqueous solutions.[5] The primary and secondary

Correspondence to: L. D. Wilson (lee.wilson@usask.ca).
Contract grant sponsors: Natural Sciences and Engineering Research Council of Canada (NSERC), the Canada Foundation for Innovation (CFI), the University of Saskatchewan.

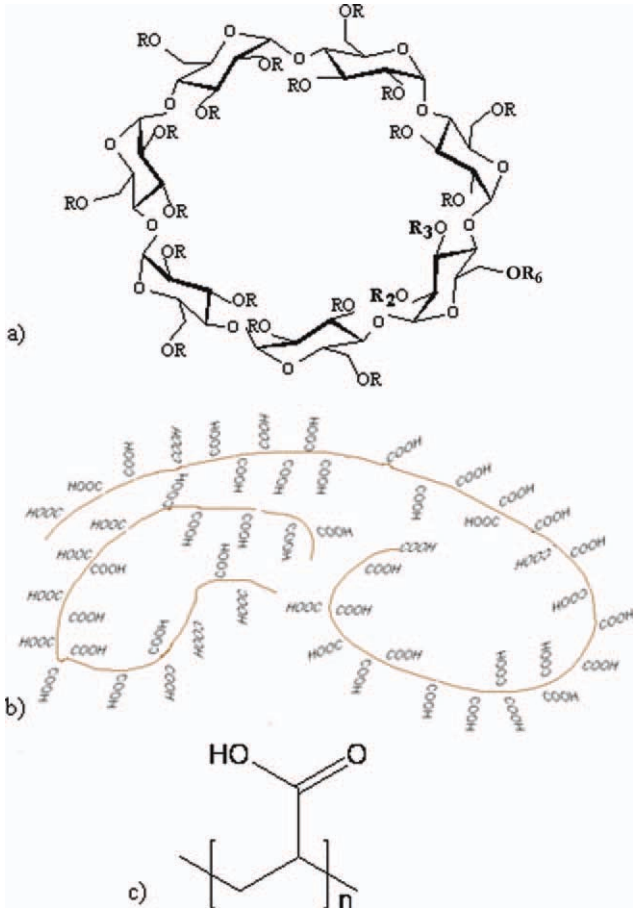

Figure 1 Molecular structure of (A) β-cyclodextrin (β-CD) where R = H at C_2-, C_3-, and C_6-OH positions. (B) Conceptual folded structure of poly(acrylic acid) (PAA), and (C) PAA monomer, where n is the degree of polymerization. [Color figure can be viewed in the online issue, which is available at wileyonlinelibrary.com.]

hydroxyl groups of β-CD are amenable to grafting onto suitable substrates such as poly(acrylic acid) (PAA), a hydrophilic mucoadhesive polymer containing numerous (56–68% w/w) carboxylic acid groups[8] [*cf.* Fig. 1(B,C)]. Copolymers derived from β-CD and PAA may serve as tunable supramolecular sorbents for the sequestration and immobilization of organic and inorganic pollutants from aqueous solution. In a previous study, CD-based microsphere polymeric materials were prepared with β-CD and PAA using a water-in-oil (w/o) micro-emulsion-evaporation method.[9,10]

The objective of this study was to prepare copolymer materials containing β-CD and PAA at various conditions (e.g., stirring rate and comonomer ratios) to evaluate changes in their physicochemical and sorption properties. This approach is anticipated to afford materials with markedly different sorption characteristics according to changes in the polymer morphology, surface area, and pore structure properties by tuning the reaction conditions. For example, the formation of β-CD grafted PAA copolymer with micro-emulsion conditions and variable cross-linking density is anticipated to yield copolymers with modified hydrophile-lipophile balance (HLB) relative to that of PAA. The surface area of the copolymer materials were characterized using N_2 adsorption and a UV-Vis dye-based sorption method in aqueous solution, respectively. The adsorbate dye (*p*-nitrophenol; PNP) was studied at variable experimental conditions (e.g., pH and concentration) and the results were evaluated using various (i.e., Langmuir, Freundlich, BET, and the Sips isotherms) models.

EXPERIMENTAL METHODS

Materials

β-cyclodextrin (β-CD), poly (acrylic acid) (PAA, Mwt. 250,000 g/mol), potassium bromide and *p*-nitrophenol (PNP) were obtained from Sigma-Aldrich Canada and used as received without any further purification. Mineral oil (heavy) and potassium phosphate monobasic were obtained from EMD. Millipore water was used to prepare aqueous solutions. Medical grade nitrogen gas (Praxair) was used as the backfill gas for the nitrogen adsorption experiments.

Synthesis of copolymer microsphere materials

β-CD hydrate (~1 g) and PAA (Mwt. 250,000 g/mol) with an accordingly variable mass ratio (1 : 3, 1 : 5, 1 : 10, 5 : 1, and 10 : 1; w/w) was utilized and the reagents were dissolved in 50 mL water. 1 : 5 water/oil emulsions were used throughout this study where 250 mL mineral oil was used in two stages (i.e., 150 and 100 mL). The first portion of mineral oil (100 mL) was pre-heated to 110–120°C in a 500-mL beaker. The aqueous solution was added to the second portion of mineral oil (150 mL) with stirring using a Corning stirrer (PC320) with dropwise addition, and the mixtures were stirred at 1100 rpm for 30 min. at ambient conditions. To prepare the copolymers at high mixing speeds, the reaction mixture was homogenized using a Power Fist rotary tool with a custom built stirring head at 13,500 rpm for an additional 10 min. The mixture was then added to the pre-heated 100 mL mineral oil at 110–120°C with stirring at 1100 rpm for 6 h until the water in the mixture was evaporated. The product and oil were cooled to room temperature, centrifuged (12,000 rpm for 10 min) and the mineral oil was decanted. 25 mL diethyl ether (5×) was then added to the product, and centrifuged (12,000 rpm for 2 min) to wash away residual mineral oil from the copolymer product. The copolymer was dried at

50°C, crushed to fine powder, and washed in a Soxhlet extractor with diethyl ether for 24 h. Finally the copolymer was dried in pistol dryer for 24 h, ground, passed through a size 40 mesh (≤0.42 mm) particle sieve, and subsequently dried under vacuum.

Characterization of copolymers

IR spectra were obtained with a Bio-RAD FTS-40 instrument and samples were analyzed in reflectance mode. Solid samples were prepared by mixing copolymers (~5 mg) with pure spectroscopic grade KBr (~50 mg) with grinding in a small mortar and pestle. The DRIFT (Diffuse Reflectance Infrared Fourier Transform) spectra were recorded at room temperature with a resolution of 4 cm^{-1} operating in the range of 400–4000 cm^{-1}. Sixteen scans were recorded and corrected against a background spectrum of pure KBr. The DRIFT spectra were recorded in the reflectance mode (Kubelka-Munk intensity units). The elemental content (w/w; %) of carbon (C) and hydrogen (H) was measured by a Perkin-Elmer 2400 CHN Elemental Analyzer with a detection limit of ± 0.3%. Solid state ^{13}C-NMR spectra with magic angle spinning (MAS) were obtained with a Varian Inova-500 operating at 125 MHz for ^{13}C. Spectra were obtained with a MAS frequency of 16 kHz in 3.2-mm vespel rotors while under $^{1}H \rightarrow ^{13}C$ CP (cross polarization) conditions with proton decoupling {^{1}H}, and external referencing to adamantane ($\delta = 38.5$ ppm) at 295 K. Thermal analyses of the copolymers were performed with a thermogravimetric analyzer, TGA (Q50 TA Instruments). Samples were heated in open aluminum pans at 30°C and allowed to equilibrate for 5 min. prior to heating at a scan rate of 5°C/min up to 500°C. The scan rate for DSC (Q50 TA Instruments) was set to 10°C per min where a dry nitrogen purge gas was used to regulate the sample temperature and the furnace compartment. DSC samples were analyzed in hermetically sealed aluminum pans over a similar temperature range. Scanning electron microscopy (SEM) images were obtained with a JEOL JSM-840A micro-imager with maximum resolution of images of 6 nm. A few granules of samples were sputter coated with gold (~200 Å thickness) with an Edwards 505 gold sputter coater using argon plasma generated with 1 kV and 30 mA for 3 min at 7.5 millibars (mb) with Ar purging during the coating process. The resulting SEM images of the samples are illustrated with a magnification of 1200× relative to the original image.

Nitrogen adsorption

Nitrogen adsorption measurements were made using a Micromeritics ASAP 2020 (Norcross, GA) to obtain the surface area and pore structure properties with an accuracy of ±5 % for the copolymers. Approximately 1 g of sample was degassed at 550 μmHg and ~70°C for several hours in the sample chamber until the outgas rate stabilized. Granular activated carbon (GAC), alumina, and silica–alumina sieves were used to check the calibration of the instrumental parameters. The BET surface area[11] was calculated from the adsorption isotherm using 0.162 nm^2 as the surface area for nitrogen gas. The micropore surface area was obtained using a *t*-plot (de Boer method).[12,13] The Barret-Joyner-Halenda (BJH) method was used to estimate the pore volume and diameter from the adsorption isotherm data.[14] The BJH method uses the Kelvin equation and the assumption of slit-shaped pores.[14]

Water swellability of copolymer materials

β-CD/PAA copolymers were placed in 3 dram glass vials containing pure Millipore water and allowed to equilibrate on a horizontal shaker table for 24 h. After the adsorption period, the materials were centrifuged in a precision semimicro centrifuge at 1550 rpm for 30 min and the supernatant water was decanted. The copolymer materials were tamped dry with a Whatman filter paper and subsequently tested using TGA from an isothermal set point of 30°C with linear heating at 5°C/min up to 200°C. The swelling ratio was determined using the following eq. (1),[15]

$$r = \frac{m(\text{swollen})}{m(\text{dry})}, \quad (1)$$

where r is the swelling ratio, m (dry), and m (swollen) are the respective masses of the copolymer before and after equilibrating with water.

Copolymer sorption study

The pore structure properties, surface area, and sorption properties were evaluated using a dye-based UV–Vis method reported previously[16,23] with PNP as the adsorbate dye. Fixed amounts (~10 mg) of the powdered and sieved copolymer materials were mixed with 7 mL of aqueous solution at variable dye concentration (0.2–10 m*M*) in 10 m*M* potassium phosphate monobasic buffer solution until fully equilibrated on a horizontal shaker table for 24 h. The buffers were prepared at pH 4.6 and 10.3, respectively, to study the sorption properties of PNP in its neutral and deprotonated forms. The initial concentration of PNP (C_o) was determined before and after sorption (C_e) with the β-CD/PAA copolymers. The estimated molar absorptivity (ε) values for PNP were determined as

follows: $\varepsilon = 9286.5$ L mol^{-1} cm^{-1} (pH= 4.6; $\lambda_{max} = 317$ nm) and $\varepsilon = 18{,}478$ L mol^{-1} cm^{-1} (pH =10.3; $\lambda_{max} = 400$ nm), in agreement with published values.[17] The sorption isotherms are depicted as plots of the adsorbed amount of PNP in the copolymer phase per mass of adsorbate (Q_e; mmol/g) versus the equilibrium residual concentration of unbound PNP in aqueous solution (C_e). The value of Q_e is defined by eq. (2) where C_o is the initial PNP concentration, V is the volume of solution, and m is the mass of sorbent.

$$Q_e = \frac{(C_0 - C_e) \times V}{m} \tag{2}$$

The dye sorption method[16] provides an independent estimate of the sorbent surface area (SA; m^2/g) in its hydrated state, according to eq. (3).

$$\mathrm{SA} = \frac{A_m Q_m L}{Y} \tag{3}$$

where A_m represents the cross-sectional area occupied by PNP (A_m for a "coplanar" orientation is 5.25×10^{-19} m^2 mol^{-1} whereas an "orthogonal" orientation is 2.5×10^{-19} m^2 mol^{-1}), Q_m is the monolayer adsorption capacity per unit mass of sorbent, L is Avogadro's number (mol^{-1}), and Y is the coverage factor ($Y = 1$) for PNP.[18]

The Freundlich, Langmuir, BET, and Sips isotherm models were used to analyze the sorption data.[19–22] The Langmuir model (*cf*. eq. 4) represents a monolayer sorption process onto a homogenous surface whereas the BET model (*cf*. eq. 5) describes multilayer adsorption processes. The Freundlich model (*cf*. eq. 6) assumes that the sorbent surface is heterogeneous in nature with an exponential distribution of active sites when an unlimited number of sorption sites are available. The Sips isotherm is a generalized isotherm model that accounts for a distribution of adsorption energies on the sorbent surface and accounts for monolayer (Langmuir) to multilayer (Freundlich) isotherms. The Sips isotherm is a relatively versatile model with several adjustable parameters where the exponent (n_s) term reflects the heterogeneity of the sorbent. When $n_s = 1$, a homogenous surface is inferred while a heterogeneous surface is inferred when $n_s \neq 1$. Langmuir isotherm behavior is predicted when $n_s = 1$, and Freundlich behavior occurs when $K_s C_e^{n_s} <<< 1$. The Langmuir, BET, Freundlich, and Sips models are defined by eqs. (4)–(7).[19–22]

$$Q_e = \frac{K_L Q_m C_e}{1 + K_L C_e} \tag{4}$$

$$Q_e = \frac{K_{\mathrm{BET}} Q_m C_e}{\left(1 - \frac{C_e}{C_s}\right)\left[1 + (K_{\mathrm{BET}} - 1)\frac{C_e}{C_s}\right]} \tag{5}$$

$$Q_e = K_F C_e^{\frac{1}{n}} \tag{6}$$

$$Q_e = \frac{Q_m K_s C_e^{n_s}}{1 + K_s C_e^{n_s}} \tag{7}$$

where K_F, K_L, K_{BET}, and K_s are the Freundlich, Langmuir, BET, and Sips equilibrium constants. C_s is the saturated aqueous solution solubility of PNP, and Q_m is defined above in eq. (3). $1/n$ is the inverse of the Freundlich exponent and is a measure of the adsorption intensity.

The criteria of the "best-fit" between the calculated isotherm and the experimental data are determined by the correlation coefficient (R^2) and the chi-square distribution (χ^2). The parameter $R^2 \sim 1$ denotes a "best-fit"; however, a more sensitive measure for nonlinear least squares fitting involves the minimization of χ^2. χ^2 is defined by eq. (8) according to the difference between the experimental ($Q_{e,i}$) and calculated ($Q_{c,i}$) sorption values toward PNP in aqueous solution.

$$\chi^2 = \sum \sqrt{\frac{(Q_{e,i} - Q_{c,i})^2}{N}} \tag{8}$$

where $Q_{c,i}$ is the calculated Q_e value with an appropriate isotherm model (*cf*. eqs. 3–6), and N is the number of experimental data points.

RESULTS AND DISCUSSION

Synthesis of copolymer materials

Microsphere β-CD-PAA copolymers were prepared using variable weight ratios of β-CD to PAA (i.e., 1 : 10, 1 : 5, 1 : 3, 5 : 1, and 10 : 1; w/w) at relatively low (1100 rpm) and high mixing speeds (13,500 rpm), respectively. The adopted notation to represent these conditions are as follows: 10 : 1_135, 5 : 1_135, and 1 : 5_135 where the ratio represents the relative comonomer mass ratio (β-CD: PAA) and the latter number designates the stirring speed, respectively. According to the different β-CD:PAA ratios, the copolymers exhibited different physical appearance, physical characteristics (e.g., thermal stability) and product morphology which varied from crystalline to amorphous powders. The relative mixing speed affects the morphology of the copolymers by altering the water droplet size in the micro-emulsion; thereby, affecting the surface area and pore structure properties of the microsphere copolymers. In contrast to the water soluble reactants, β-CD and PAA, the copolymer products are generally insoluble. The insolubility of copolymers in water is an important property for the design of sorbents for the study of solid-solution sorption equilibria, as outlined herein.

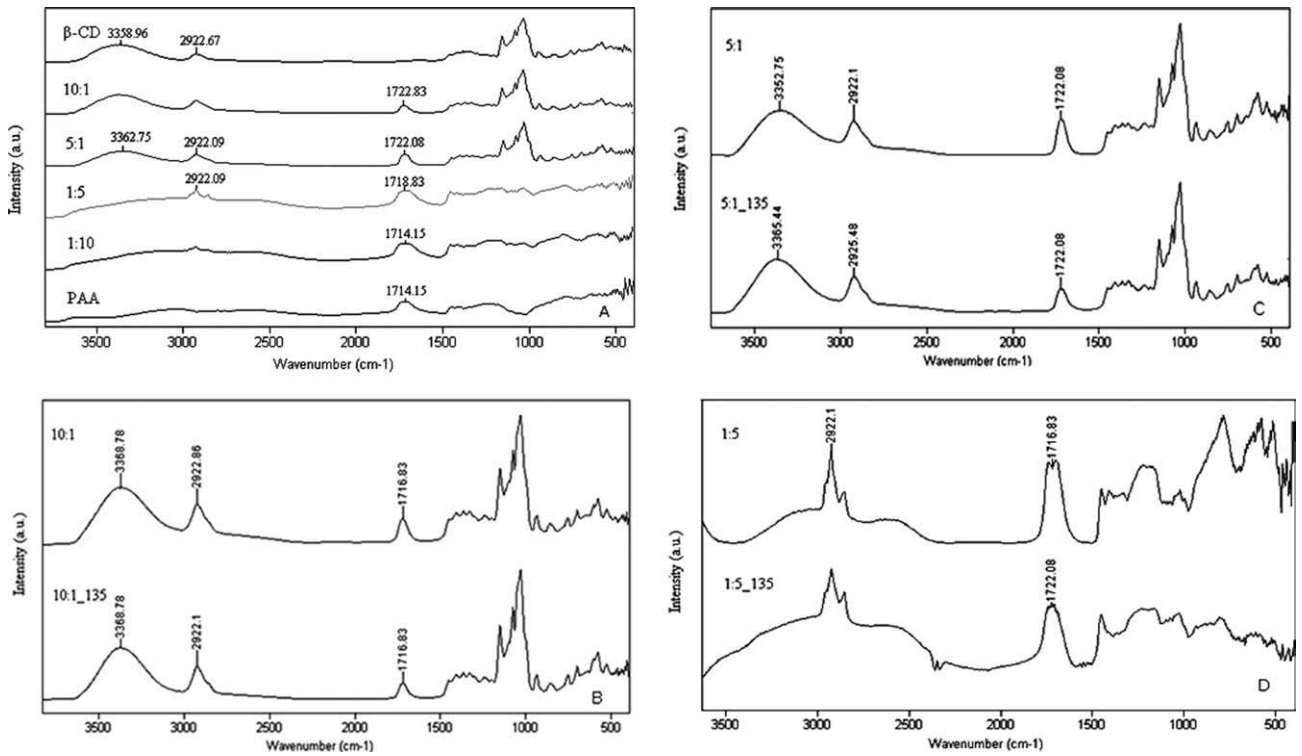

Figure 2 IR spectra (DRIFTS) for (A) β-CD and 1 : 10, 1 : 5, 10 : 1, and 5 : 1 β-CD:PAA copolymers at room temperature, (B) 10 : 1 and 10 : 1_135 β-CD:PAA copolymers using low and high mixing speeds (1, 100, and 13,500 rpm), respectively (C) 5 : 1 and 5 : 1_135 β-CD:PAA copolymers, and (D) 1 : 5 and 1 : 5_135 β-CD:PAA copolymers.

Characterization of copolymer materials

The FT-IR spectra for the starting materials (β-CD and PAA) and the β-CD:PAA copolymers (10 : 1, 5 : 1, 1 : 5, and 1 : 10) are shown in Figure 2(A). The –OH (~3400 cm^{-1}), -CH (~2900 cm^{-1}) and ─C═O (~1700 cm^{-1}) stretching regions are present in the copolymer products and confirm their molecular identity. The IR spectra for the copolymers generally represent additive features of the characteristic functional groups present in the starting materials. However, each copolymer has ─C═O band (~1730 cm^{-1})

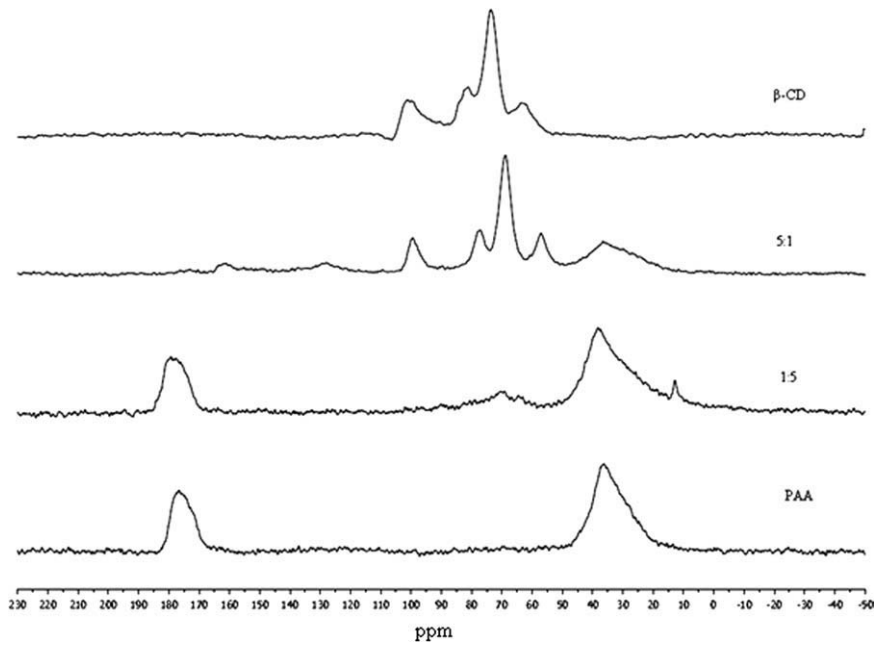

Figure 3 ^{13}C-NMR CP-MAS spectra for β-CD, 5 : 1 and 1 : 5 β-CD:PAA copolymers, and PAA at 295 K.

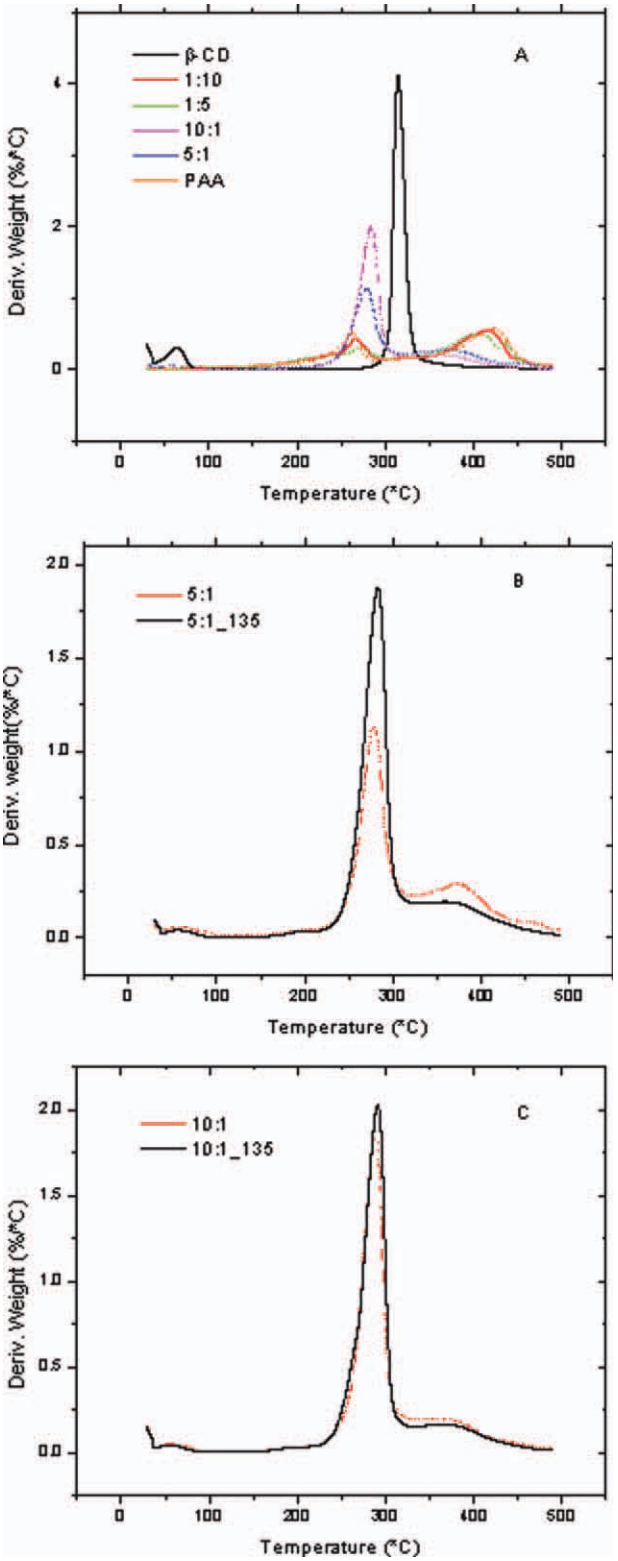

Figure 4 (A) TGA of β-CD, PAA, and β-CD/PAA copolymers 1 : 10, 1 : 5, 10 : 1, and 5 : 1 (w/w). (B) β-CD/PAA copolymers 5 : 1 and 5 : 1_135 using low and high mixing speed (1100, and 13,500 rpm, respectively). (C) β-CD/PAA copolymers 10 : 1 and 10 : 1_135 using low and high mixing speed (1,100 and 13,500 rpm, respectively). [Color figure can be viewed in the online issue, which is available at wileyonlinelibrary.com.]

due to the formation of the ester linkage between β-CD and PAA [*cf.*, Fig. 2(A)], which agrees with previous reports.[23,24] The —C=O vibrational band is relatively broad for the copolymers as compared to β-CD, especially for the copolymers with greater PAA content (1 : 5 and 1 : 10). A possible reason may be the overlap of the IR signatures for the unreacted carboxylic groups of PAA (-COOH) and the crosslinked ester (-COOR; R = β-CD) linkages of the grafted PAA. The carbonyl band (~1700 cm^{-1}) also shows a shift in frequency that varies according to the β-CD:PAA comonomer ratio. Generally, the IR spectra of copolymers 10 : 1 and 5 : 1 tend to resemble the spectral features observed for β-CD hydrate whereas the 1 : 5 and 1 : 10 spectra tend to resemble the broad spectral features of PAA (~2900 cm^{-1}, ~1700 cm^{-1}, and 1500–500 cm^{-1}). The broad features relate to the polydisperse nature of the PAA polymers and its amorphous structural characteristics. The copolymer products obtained from preparations at the various mixing speeds do not reveal any major differences amongst copolymers with similar β-CD:PAA ratios (i.e., 10 : 1 and 10 : 1_135, 5 : 1 and 5 : 1_135, and 1 : 5 and 1 : 5_135), as evidenced in Figure 2(B–D). A notable difference is the relative intensity changes of the —C=O to —OH vibration bands for the copolymers prepared at high vs. low speed mixing conditions, respectively. The —C=O band shows a reduced intensity for the copolymers prepared at high mixing speeds.

Figure 3 illustrates the ^{13}C CP-MAS NMR spectra of the 5 : 1 and 1 : 5 β-CD:PAA copolymers, along with the comonomers, β-CD hydrate, and PAA. Although each glucose unit of β-CD contains six unique ^{13}C atoms per glucose residue, the spectra for the copolymers in Figure 3 reveal approximately four unique ^{13}C-NMR lines between 60 and 110 ppm due to the overlap of some of the individual ^{13}C resonance lines, in agreement with a previous report[31].

TABLE I
Experimental[1] and Calculated[2] Comonomer (β-CD: PAA) Ratios

β-CD:PAA Copolymers (w/w)	Experimental value[b] (β-CD:PAA)	Calculated value[c] (β-CD:PAA)	χ^{2a}
1 : 10	14 : 1	22 : 1	0.00005
1 : 5	42 : 1	44 : 1	0.00033
10 : 1	239 : 1	2203 : 1	0.00252
10 : 1_135	302 : 1	2203 : 1	0.00554
5 : 1	122 : 1	1101 : 1	0.00043
5 : 1_135	239 : 1	1101 : 1	0.00262

[a] χ^2, Chi-square distribution.
[b] Experimental values (mole ratio obtained from TGA deconvolution results).
[c] Calculated values (mole ratio obtained from mass ratios of β-CD/PAA from the reactants used in the synthesis).

TABLE II
Calculated Elemental Composition (C and H (w/w %)) for β-CD and PAA and Elemental (C, H) Micro-Analyses For Various Copolymers Prepared at High (5 : 1, 1 : 5) and Low (5 : 1_135, 1 : 5_135) Mixing Speeds, Respectively

	PAA (calc.[a])	β-CD (calc.[a])	5 : 1	5 : 1_135	1 : 5	1 : 5_135
%C	50.0	44.4	46.1	45.8	48.3	48.2
%H	5.56	6.17	7.14	6.97	6.29	6.32

[a] The calculated elemental composition was based on known molecular weight and formula of the molecules.

Similar ^{13}C-NMR signatures observed in Figure 3 for β-CD are similarly noted for the 5 : 1 and 1 : 5 copolymer materials, especially for the copolymers with greater β-CD content. The β-CD macrocycle in copolymer materials is covalently grafted onto the PAA polymer chain as a pendant group via an ester linkage via the primary C6-OH groups of β-CD (*cf.*, Fig. 1) because of its greater reactivity relative to the secondary (i.e., C2- and C3-OH) hydroxyl groups. Thus, β-CD is tethered to the polymer chain at one or more hydroxyl groups which facilitates sufficient motional dynamics that contribute to the observed narrow lines, as compared with other types of conventional cross-linked copolymer materials.[23] The carbonyl signature (~170–183 ppm) for the copolymer materials is attributed to the numerous carboxylic acid and ester groups along the PAA backbone. The reduced NMR intensity of the carbonyl signature for the 5 : 1 copolymer is attributed to a reduction in cross polarization due to esterification (—COOR) of the carboxylic acid (—COOH) groups of PAA and changes in the hydration state of the material. The presence of an adjacent H atom in the —COOH groups with variable hydration contributes to variable cross polarization transfer (H→C) dynamics. Compared with the sharp resonance lines of β-CD hydrate, the broad ^{13}C resonance lines for the aliphatic signatures (~15–50 ppm) of the PAA backbone are related to the variable conformation of aliphatic chain and contributions arising from the polydisperse chain length distribution of PAA. The broad resonance lines of the subunits for the β-CD:PAA copolymers illustrate the amorphous character of the materials, according to an ensemble of molecular environments due to random attachment of the comonomers. The foregoing ^{13}C CP-MAS NMR results are consistent with grafted copolymer materials containing β-CD and PAA.[10]

In Figure 4, the TGA results are presented as the derivative weight (mass loss/temperature) against temperature for the copolymers and comonomers, respectively. Different thermal profiles are observed for the various copolymers as the relative monomer content is varied. Accordingly, the TGA results for the copolymers show two thermal events near 275 and 400°C, respectively. The mass loss corresponds to the decomposition of the respective comonomers (i.e., β-CD and PAA) at their respective thermal decomposition temperatures. The relative mole ratios of β-CD and PAA were estimated by deconvolution of the thermal events of the tabulated peak areas in Table I. As the β-CD composition of the copolymer increases, the area corresponding to the thermal event ~275°C increases. Similarly, the integrated area ~400°C increases as the PAA content of the copolymer increases. The relative peak areas

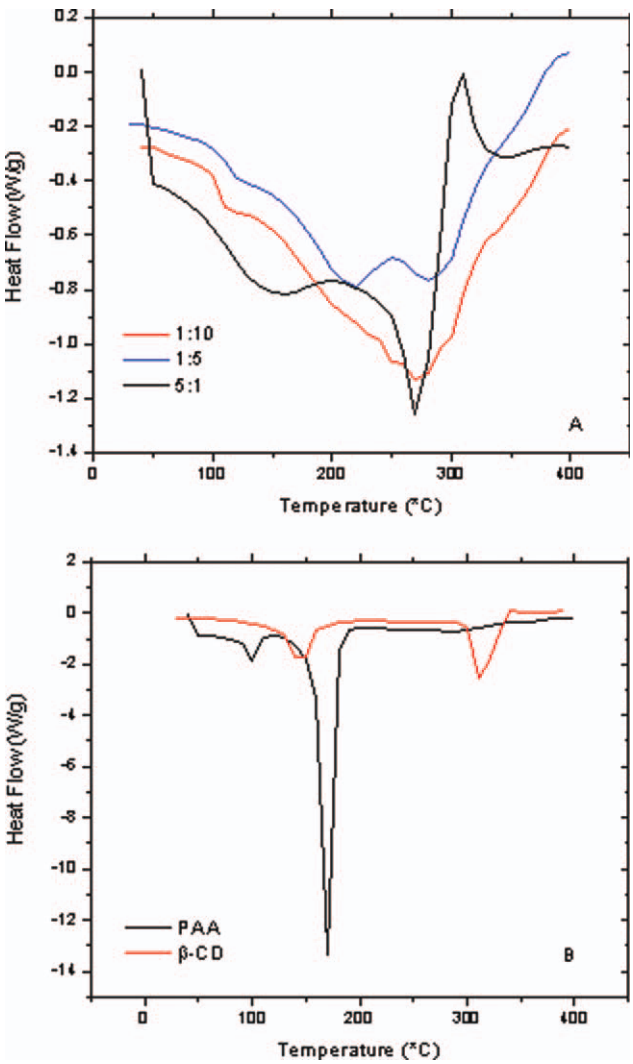

Figure 5 DSC thermograms of (A) 1 : 10, 1 : 5, 10 : 1, and 5 : 1 β-CD:PAA copolymers and (B) β-CD and PAA in the temperature range 35–450°C obtained with a scan rate of 10°C/min. [Color figure can be viewed in the online issue, which is available at wileyonlinelibrary.com.]

TABLE III
BET Surface Area Estimates For the β-CD:PAA Copolymer Materials and Comonomers (β-CD and PAA) Obtained Using N_2 Adsorption at 77 K

Sorbent materials	10 : 1	10 : 1_135	5 : 1	5 : 1_135	1 : 5	1 : 3	β-CD	PAA
Surface area[a] (m^2/g)	4.47	3.90	1.63	0.970	0.275	0.287	1.20	0.376

[a] According to N_2 adsorption at 77 K with the use of a linearized BET model.

observed in Figure 4 correlate with the observed intensity change for the IR results for each comonomer subunit. In Figure 4(B), the copolymers prepared at high speed conditions show greater β-CD content relative to slower mixing speed conditions (e.g., 5 : 1 and 5 : 1_135). Notwithstanding the presence of trace solvent residues in the copolymer sorbents, the results are in general agreement with the C and H elemental micro-analyses (*cf.*, Table II).[27] Based on the IR, TGA, and the elemental micro-analyses, a greater amount of β-CD was grafted onto the PAA at higher mixing speed conditions. The higher mixing speeds produce greater internal pressure within the water droplets of the w/o micro-emulsion, and provide further support for the observed effects. The higher mixing speeds produce smaller droplets and favor these types of condensation reactions.[16,17] The relative offset in the grafting efficiency of β-CD onto PAA is less apparent at 10 : 1 vs. 5 : 1 copolymers at variable spinning speed; however, this can be related to increased steric effects as the PAA chain becomes increasingly grafted. The β-CD content of the grafted copolymer materials are observed to adopt the following order: 10 : 1_135 ~ 10 : 1 > 5 : 1_135 > 5 : 1> 1 : 5_135 > 1 : 5 > 1 : 10 (w/w).

The DSC plots shown in Figure 5 indicate that the copolymers have modified thermal stability relative to the co-monomers (PAA and β-CD), as anticipated

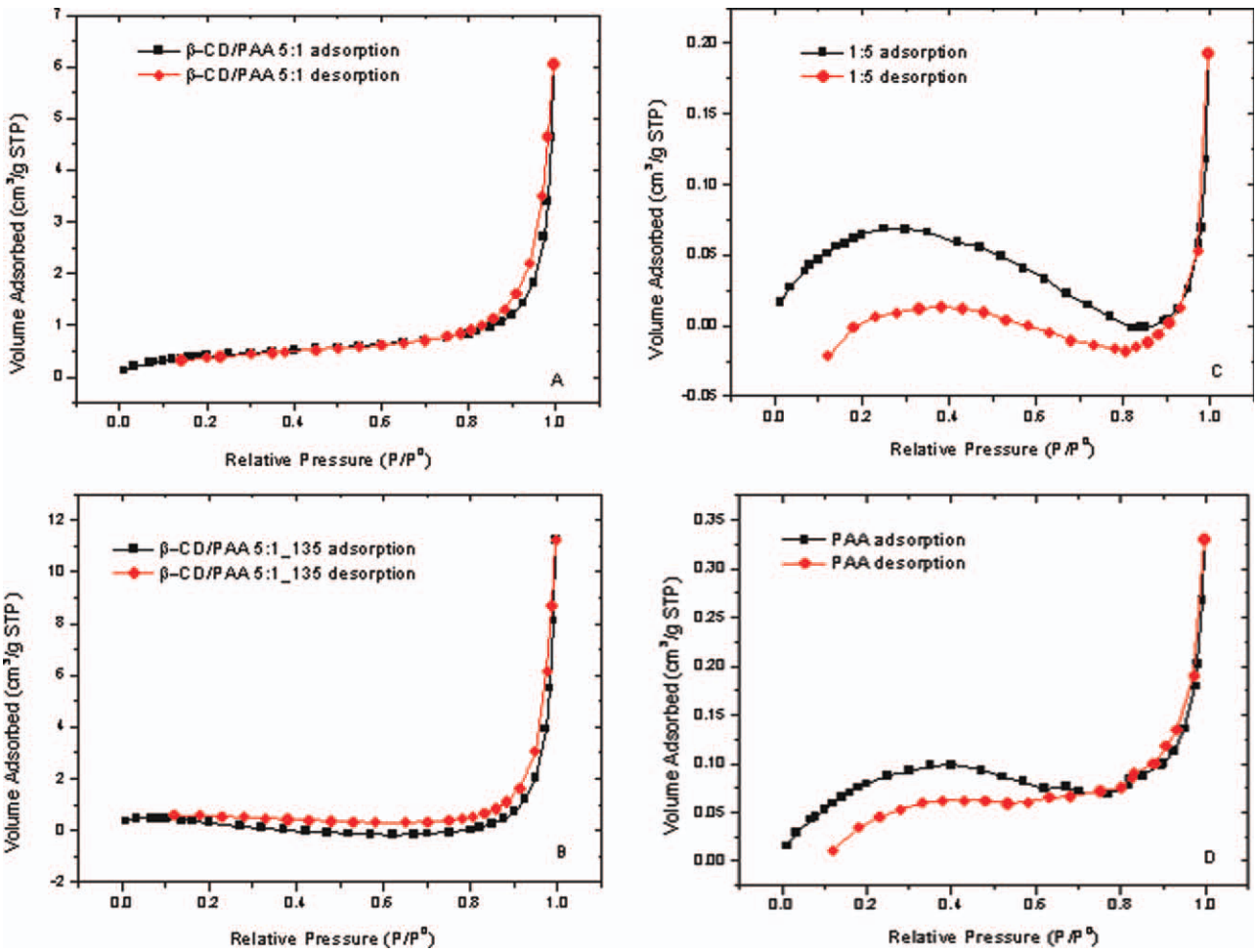

Figure 6 Nitrogen adsorption-desorption isotherm for β-CD:PAA copolymers materials and their starting materials at 77 K: A: 5 : 1 β-CD:PAA; B: 5 : 1_135 β-CD:PAA; C: 1 : 5 β-CD:PAA; and D: PAA. [Color figure can be viewed in the online issue, which is available at wileyonlinelibrary.com.]

for cross-linked copolymer materials. The greater temperature onset for the PAA comonomer in the copolymer material illustrates that the thermal stability of PAA is enhanced. The grafted copolymer is anticipated to display different morphology relative to PAA because grafting of β-CD onto the —COOH surface groups will affect the packing and intermolecular interactions between adjacent copolymer chains in the solid state. The broadened thermal transitions for the copolymers and the broader ^{13}C-NMR signatures provide evidence that the copolymer material is amorphous in nature. The incremental grafting of β-CD onto PAA increases the molecular weight of the copolymer and alters its thermophysical properties in a corresponding manner, as evidenced from the DSC results of Figure 5.

Nitrogen adsorption

The sorption properties of the copolymer materials in the solid state were studied by nitrogen porosimetry (*cf.*, Table III). Figure 6(A–D) illustrates the nitrogen adsorption–desorption isotherms β-CD/PAA copolymers and the PAA precursor. The copolymers show the hysteresis loops which represent Type IV isotherms. Type IV isotherms generally describe the monolayer-multilayer adsorption of microporous adsorbents.[25] The corresponding hysteresis loops feature parallel and almost horizontal branches (Type H1 and H3) and have been attributed to adsorption–desorption in narrow slit-like pores that are often associated with narrow pore size distributions.[25] The BET surface area estimates for 10 : 1 and 10 : 1_135 are 4.47 and 3.90 m^2/g, respectively. The copolymers with high PAA content (1 : 5) yielded lower BET surface area (0.275 m^2/g); whereas, the 1 : 3 β-CD:PAA copolymer was slightly greater (0.287 m^2/g). The magnitude of the BET estimates obtained herein are of similar magnitude to those for 1 : 22 β-CD-epichlorohydrin copolymers (~0.2 m^2/g, BET).[26] A contributing factor for the attenuated surface areas may originate from the disordered and collapsed copolymer framework in the anhydrous state, and the reduced accessibility of the micropores in the copolymer framework. At low β-CD content, the PAA copolymer forms a more densely packed framework. In contrast, copolymers with greater β-CD content may have reduced packing density which result in the formation of micropore sites, evidenced by the greater sorption of N_2 in such materials. The high speed copolymer materials (10 : 1_135) show attenuated sorption toward nitrogen relative to the copolymers prepared at reduced mixing speed (10 : 1) because of the greater crosslink density and reduced pore size of the 10 : 1_135 material, described above. Similarly, the highly cross-linked and dense framework structure attenuates the accessibility of nitrogen gas. Additionally, PAA is considered a "soft material" with significant conformational motility of the PAA backbone. This results in a fairly low BET surface area (0.376 m^2/g) in the solid state since the polymer likely adopts a collapsed micropore structure with reduced surface area, as compared to the hydrated copolymer in aqueous solution.[27]

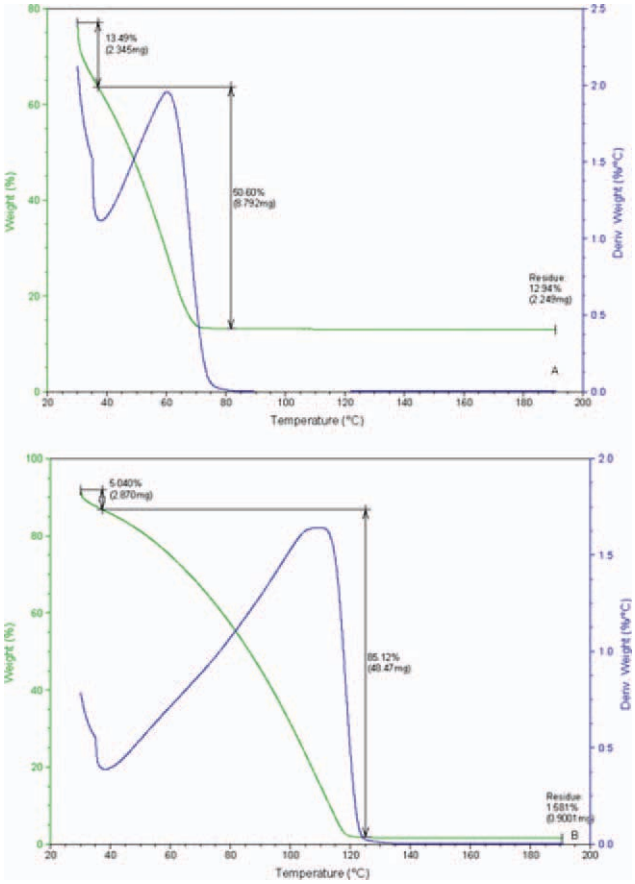

Figure 7 TGA of β-CD:PAA copolymers for analysis of water swelling properties: (A) 5 : 1 β-CD:PAA copolymer and (B) 1 : 5 β-CD:PAA copolymer equilibrated in Millipore water for 24 h and at 295 K. [Color figure can be viewed in the online issue, which is available at wileyonlinelibrary.com.]

Water swellability studies

The occurrence of potential swelling of the copolymer framework in aqueous solution motivated a study of the swelling property of such materials.[28] The swelling properties of the 5 : 1 and 1 : 5 β-CD:PAA copolymers were studied in water using a TGA-based method [*cf.*, Fig. 7(A,B)]. The copolymer with greater PAA content (1 : 5 β-CD:PAA) shows greater swelling than the 5 : 1 β-CD:PAA copolymer. The greater swelling of the 1 : 5 copolymer is attributed to the higher PAA content and its hydrophilic characteristics. The swelling ratio was calculated from the gravimetric loss using TGA

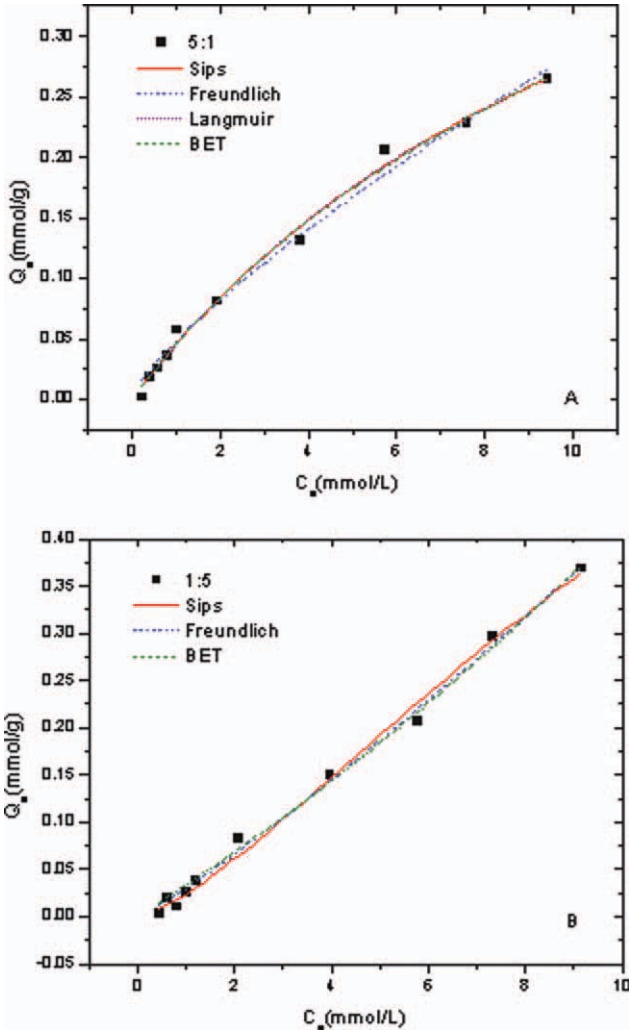

Figure 8 Sorption isotherm for β-CD:PAA copolymers (A) 5 : 1 β-CD:PAA, $n_s = 1.0$ and (B) 1 : 5 β-CD:PAA, $n_s = 1.4$ with various isotherms: Sips, Freundlich, Langmuir, and BET models. [Color figure can be viewed in the online issue, which is available at wileyonlinelibrary.com.]

results and eq. (1). After 24 h of equilibrium swelling in deionized water, the hydrated 1 : 5 polymer was observed to have a swelling ratio $r = 59$ and the 5 : 1 β-CD:PAA had a value of $r = 5$. The results show that the 1 : 5 β-CD/PAA adsorbs ~59 times the amount of water relative to its mass. In contrast, the 5 : 1 β-CD/PAA copolymer adsorbs approximately four times its weight in water relative to its dry mass. In Figure 7, the desorption temperature of water for the 5 : 1 β-CD:PAA copolymer is ~60°C, indicating that adsorption occurs mainly on the surface sites. In contrast, the 1 : 5 copolymer has a wider temperature range of desorption (~40–120°C) where the maximum water desorption occurs ~110°C. Water is adsorbed at both the surface and micropore framework sites of the 1 : 5 copolymer. The increased swelling of the copolymers with greater PAA content may result from the favorable hydration of the —COOH groups. Such hydration effects are anticipated to contribute to morphological changes and surface area effects due to swelling of the copolymer framework.[28]

Copolymer sorption studies

Sorption properties at pH 4.6

The sorption properties of the copolymer materials were studied at 22°C with PNP as the adsorbate molecule, below and above the pK_a for PNP (pH 4.6 and 10.3), respectively, in aqueous solution. The decoloration of PNP in the supernatant solution was monitored at equilibrium in solutions containing fixed amounts of copolymer. The absorbance of PNP ranged from yellow to various levels of decolorization over the concentration range investigated at pH 4.6. At similar conditions, the inclusion of PNP by β-CD results in the enhancement of the molar

TABLE IV
Equilibrium Sorption Parameters Obtained from the Adsorption of PNP by β-CD:PAA Copolymer Materials at pH 4.6 and 295 K, According to Various Isotherm Models

Isotherm models	Parameters	5 : 1	5 : 1_135	1 : 5	1 : 5_135
Langmuir	Q_m (mmol/g)	0.632	–	–	–
	K_L (L/mmol)	0.0766	–	–	–
	R^2	0.994	–	–	–
	χ^2	7.00×10^{-5}	–	–	–
BET	Q_m (mmol/g)	0.478	1.66	2.19	15.7
	K_{BET} (Lmmol/g^2)	8.29	1.87	1.55	0.186
	R^2	0.996	0.996	0.995	0.994
	χ^2	0.0182	0.0263	0.0302	0.0345
Sips	Q_m (mmol/g)	0.613	0.872	1.12	1.32
	K_{Sips} (L/mmol)	0.0809	0.0667	0.0646	0.0591
	n_s	1.0	1.2	1.4	1.5
	R^2	0.994	0.990	0.994	0.988
	χ^2	8.00×10^{-5}	1.30×10^{-4}	1.20×10^{-4}	2.30×10^{-4}
Freundlich	K_F (mmol/g)	0.0480	0.0375	0.0299	0.0253
	$1/n$	0.775	0.964	1.14	1.22
	R^2	0.990	0.992	0.995	0.993
	χ^2	1.10×10^{-4}	1.10×10^{-4}	9.00×10^{-5}	1.50×10^{-4}

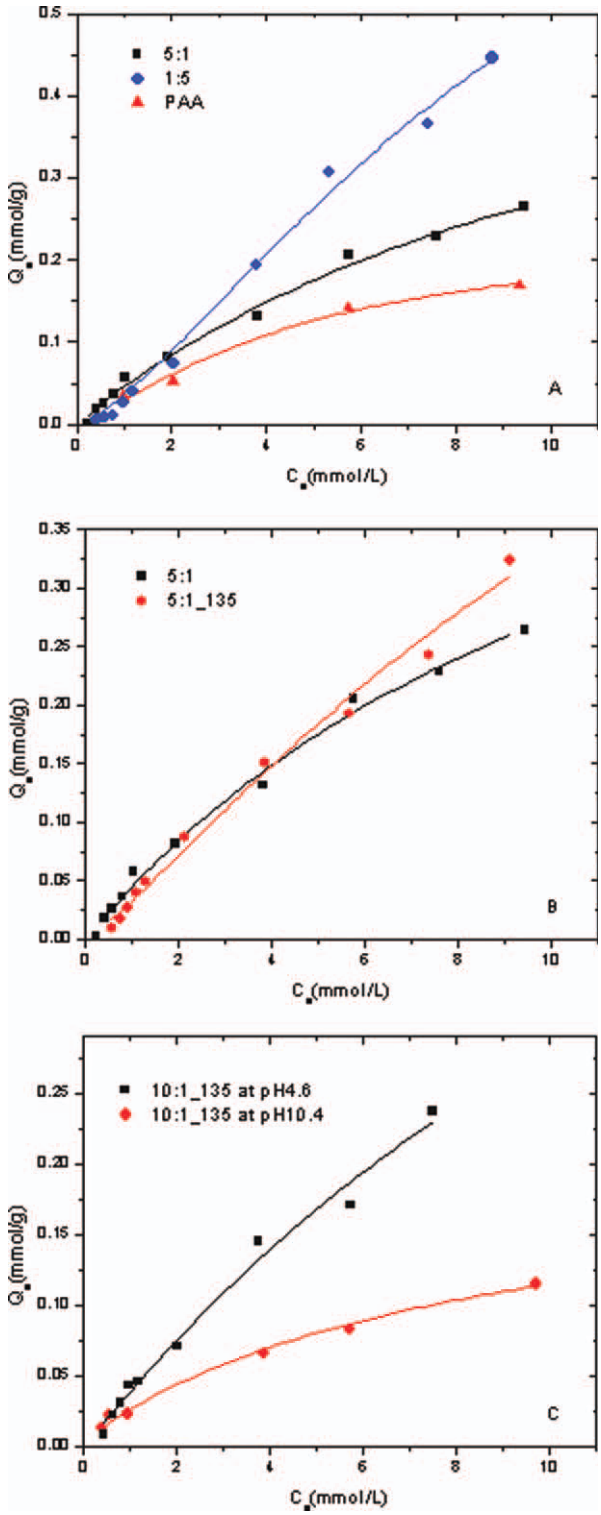

Figure 9 Sorption isotherm for β-CD:PAA copolymers with a fixed mass of sorbent (~10 mg) and varying concentrations of PNP at 22°C: (A) PAA and both 1 : 5 and 5 : 1 β-CD:PAA copolymers at pH 4.6; (B) Copolymers prepared at various mixing speeds, low speed 5 : 1 and high speed, 5 : 1_135 at pH 4.6; (C) Copolymer 10 : 1 at pH 4.6 and pH 10.3. The best-fit results were obtained using the Sips isotherm. [Color figure can be viewed in the online issue, which is available at wileyonlinelibrary.com.]

absorptivity of the dye in aqueous solutions. The attenuation observed in the case of the β-CD:PAA copolymer materials was related to the unique intermolecular interactions between the PAA comonomer and PNP.

In Figure 8, the sorption isotherms (Q_e vs. C_e) are shown for the 5 : 1 and 1 : 5 β-CD:PAA copolymers at pH 4.6. In general, the magnitude of Q_e increases monotonically with increasing C_e. The isotherms for the 5 : 1, 1 : 5, 5 : 1_135, and 1 : 5_135 β-CD:PAA copolymers were analyzed by various models, described by eqs. (4–7). The best-fit parameters obtained from each model are listed in Table IV. The Langmuir model generally showed unsatisfactory fits except for the 5 : 1 β-CD/PAA copolymer. In contrast, the BET isotherm provides a more suitable fit to the sorption data; however, greater χ^2 values are observed (*cf.* Table IV). The Sips isotherm provides a good general description of the sorption behavior for each of the copolymers, and the n_s parameter provides an estimate of the surface heterogeneity. Monolayer (i.e., Langmuir) adsorption behavior is observed for isotherms when $n_s = 1$, according to the Sips isotherm. The 5 : 1 copolymer yields a heterogeneity parameter ($n_s = 1$) and reasonable agreement is observed with the three isotherms (Langmuir, BET, and Sips); whereas, poor agreement is observed for the Freundlich model. Heterogeneous sorption sites are concluded as the value of n_s deviates from unity. In copolymer materials, heterogeneous sorption ($n_s \neq 1$) may occur because of the occurrence of inclusion and noninclusion binding sites. In Table IV, the 1 : 5 copolymers

TABLE V
Dye-Based Estimates of the Surface Area (SA) For Polymeric Materials Obtained For the Sorption of PNP at 295 K and pH 4.6 and 10.3 Including the Best-Fit Parameters (Q_m, K_{Sips}, and n_s) According to the Sips Isotherm

Copolymer	pH	SA[a]	Q_m[b]	K_{Sips}[c]	n_s	χ^2[d]
10 : 1	4.6	54.0	0.359	0.185	1.3	0.00002
5 : 1	4.6	92.2	0.613	0.0809	1.0	0.00008
1 : 3	4.6	165	1.10	0.0509	1.3	0.00013
1 : 5	4.6	169	1.12	0.0646	1.4	0.00012
1 : 10	4.6	331	2.20	35.5	1.5	0.0403
10 : 1_135	4.6	67.1	0.447	0.129	1.2	0.0285
5 : 1_135	4.6	131	0.872	0.0667	1.2	0.00013
1 : 5_135	4.6	199	1.32	0.0591	1.5	0.00023
PAA[e]	4.6	36.2	0.240	0.216	1.3	0.00015
5 : 1_135	10.3	12.0	0.0701	0.277	1.2	0.00002
10 : 1_135	10.3	28.8	0.191	0.147	1.0	0.00003

[a] Surface area, (m^2/g).
[b] Q_m, (mmol/g).
[c] K_{Sips}, (L/mmol).
[d] χ^2, Chi-square distribution.
[e] PAA was test at both pH 4.6 and 10.3, with no observable sorption at pH 10.3.

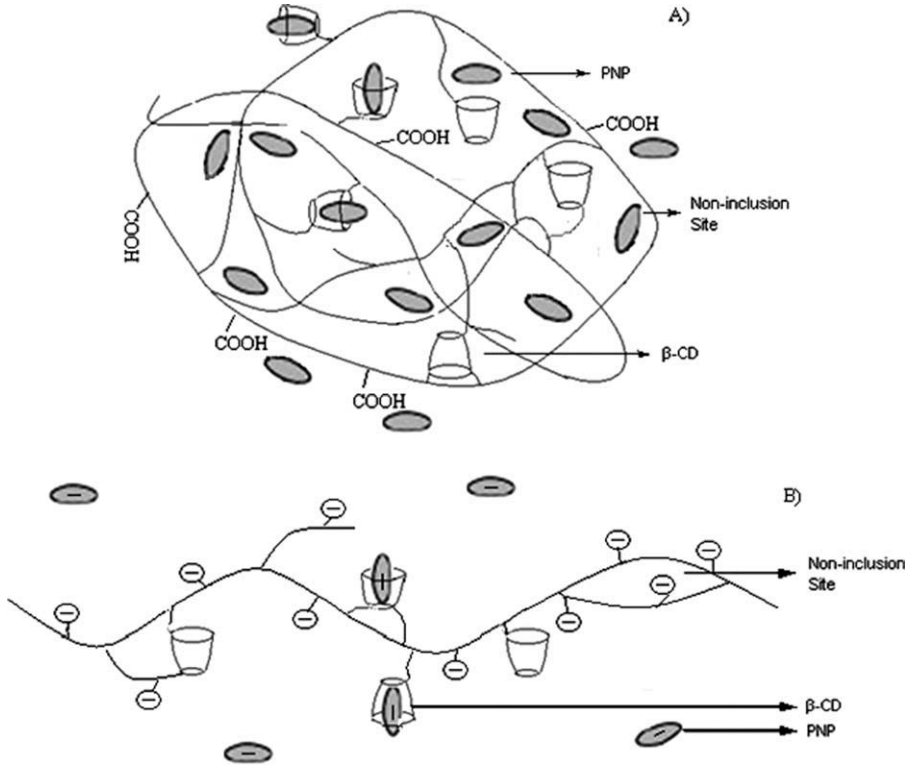

Scheme 1 Conceptual structure of a cross linked β-CD:PAA copolymer containing an adsorbed guest molecule (oval) within the β-CD inclusion sites (tori interior) and the noninclusion sites (PAA surface) of the copolymer framework: (A) pH 4.6 (pH < pK_a PAA) and (B) pH 10.4 (pH > pK_a PAA). The straight line segments connecting the β-CD tori represent the ester linkage. The solvent has been omitted for clarity.

[$n_s = 1.4$, *cf.* Fig. 8(B)], 1 : 5_135 ($n_s = 1.5$), and 5 : 1_135 ($n_s = 1.2$) are well-described by the Freundlich model because it accounts for such heterogeneous adsorption processes. Over the range of dye concentrations examined, the saturation of the 1 : 5 β-CD:PAA copolymer is not achieved. There are multiple sorption sites if one considers the potential contribution of the β-CD (inclusion) sites and the PAA surface (noninclusion) sites of the PAA backbone. In Figure 8(B), the 1 : 5 β-CD:PAA copolymer does not show saturation of the sorption sites when C_e reaches ~10 m*M*. In general, the Sips isotherm model shows favorable agreement with the observed sorption results of copolymers. In addition to the heterogeneity parameter (n_s), the K_{Sips} parameter provides insight about the sorption affinity between the sorbent and PNP. The Sips isotherm was the preferred model to describe the overall sorption behavior for the systems in this study because of its versatility in describing monolayer- to multilayer-type sorption phenomena, according to the overall goodness-of-fit observed.

Figure 9(A) shows the Sips isotherm (Q_e vs. C_e) results for the 5 : 1 and 1 : 5 β-CD:PAA copolymer and PAA at pH 4.6. The value of Q_e increases monotonically as C_e increases. The sorption data were fit using the Sips isotherm (*cf.*, eq. 7) and the "best-fit" sorption parameters for this model are listed in Table IV. In Table V, the dye-based SA estimates of the copolymers were estimated using Q_m (Table V) and eq. (3). The values in Table V range from 54.0 m^2/g to 331 m^2/g at pH 4.6 and are two orders of magnitude greater than the BET SA values in Table III. This difference is attributed to the occurrence of swelling which was previously observed in urethane copolymers containing β-CD[28]. The β-CD:PAA copolymers display a relatively wide range of sorption capacities toward PNP according to the values of Q_m (0.359–2.20 mmol/g) for these conditions. The sorption properties are related to the preparative (comonomer mole ratio and mixing speed) conditions of the copolymers and may be tuned accordingly. The values of Q_m fall in the range observed for β-CD epichlorohydrin copolymers (0.296 mmol/g)[29] and surface modified activated carbon materials containing β-CD (2.58 mmol/g)[30]. At pH 4.6, the sorption capacity varied amongst the various β-CD/PAA the copolymers, as follows: 1 : 10 > 1 : 5 > 1 : 3 > 5 : 1 >10 : 1 (w/w). The increasing magnitude of Q_m correlates with increasing PAA content of the copolymer materials. There are several factors that contribute to the observed differences; increased number of —COOH groups of PAA favor H-bonding with PNP, and reduced

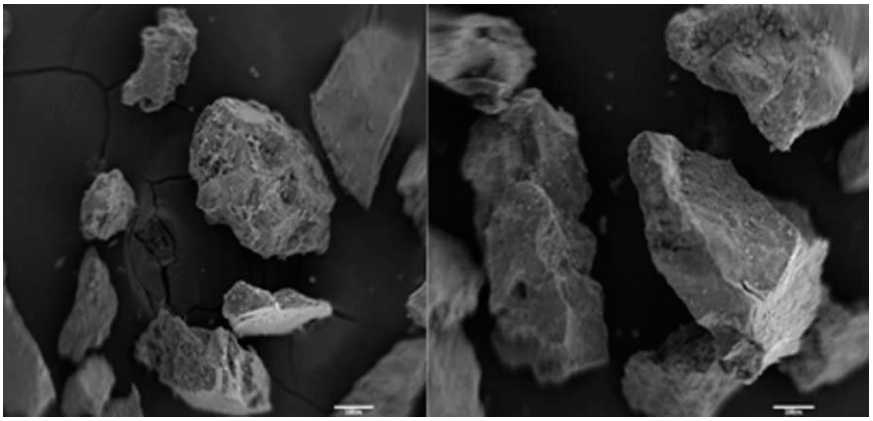

Figure 10 SEM image of β-CD/PAA copolymers 1 : 3(w/w) with a scale bar = 100μm, and magnification of 1200×.

grafting affects the surface area of the sorbent material.[31] The mixing speed affects the sorption properties of the copolymers [*cf.*, Fig. 9(B)] because greater mixing speed dramatically increases the accessible surface area as evidenced in the following trend for Q_m: 10 : 1_135>10 : 1; 5 : 1_135>5 : 1. Two factors which account for the observations are the surface accessibility of the sorption sites toward PNP and the aforementioned grafting efficiency with increasing mixing speed.

Sorption properties at pH 10.3

Figure 9(C) illustrates a comparison of the copolymer 10 : 1_135 sorption isotherms at pH 10.3 and 4.6 at 22°C. There are significant differences between the two isotherms and the "apparent" surface area of the copolymer materials are attenuated (SA~12.0 m^2/g to ~28.8 m^2/g) above the pK_a of PNP. The copolymers have greater sorption at pH 4.6 compared with pH 10.3 because PAA is deprotonated resulting in negatively charged surface sites. The ionization of the —COOH side groups along the polymer backbone of PAA ($pK_a \sim 4.5$) cause coulombic repulsions with the anion form of PNP ($pK_a = 7.14$), as it is the prevalent form at pH 10.3.

In general, the copolymer materials with greater PAA content (reduced crosslink density) and higher mixing speeds are concluded to have greater sorption capacity at pH 4.6. This is understood in terms of favorable H-bonding interactions between PNP and with the carboxylic groups along the PAA polymer backbone along with van der Waals interactions in the micropore sites of the copolymer framework. At pH 10.3, the inclusion sites are favored since the coulombic repulsion between the carboxylate groups of PAA and the anion form of PNP are shielded when bound by β-CD. The enhanced binding affinity of PNP at alkaline conditions was independently observed in a recent study (*cf.*, Table III in Ref. 32).[32] The sorption of PNP by the β-CD:PAA copolymers at different pH (4.6 and 10.3) are shown in Scheme 1. There are two potential sorption sites on the β-CD:PAA copolymer framework when $pH \leq pK_a$ (PAA) due to the availability of the β-CD inclusion sites and the PAA surface domains (noninclusion). The copolymers with low PAA (high β-CD) content show a monolayer adsorption with $n_s \sim 1$ indicating that the β-CD inclusion sites are independent and may play a dominant role in sorption processes (i.e., 5 : 1 copolymer). Copolymers with reduced levels of grafting show favorable sorption at the noninclusion sorption sites and yield nonunitary values for the heterogeneity parameter ($n_s \neq 1$). The pH may dramatically change the framework morphology of the copolymers, especially for the copolymers with low β-CD content. At pH 10.3, $pH > pK_a$ (PAA), and the presence of negatively charged carboxylate groups on PAA result in coulombic repulsion with the anion form of PNP, and the sorption capacity of the copolymer is attenuated.

Compared to porosimetry-based methods, the PNP-based sorption in aqueous solution provides a much greater "apparent" surface area for copolymer sorbents. This effect results from hydration-induced swelling of the copolymer framework in aqueous solution.[27] The dye-based method monitors changes in the absorbance of PNP related to sorption by the copolymer sorbent. The SEM images in Figure 10 do not show evidence of meso- or macro-porous structures in the solid state, in agreement with the gas adsorption results. The SEM results reveal a microporous material with limited pore structure characteristics. The occurrence of swelling strongly affects the accessibility of adsorptive probes in the anhydrous vs. hydrate states because of the hydration dependent morphology and variable sorption properties of the copolymer material.

CONCLUSIONS

In this work, a range of copolymer materials were prepared and their sorption properties were characterized in aqueous solution with *p*-nitrophenol at 295 K and nitrogen adsorption in the solid state at 77 K. The copolymers show a range of physicochemical properties characteristic of amorphous powders to crystalline materials in the solid state, corresponding to the relative comonomer ratios and the mixing speed employed in the synthesis. In aqueous solution, the copolymers display variable swelling properties in aqueous solution. The Sips model provided the best overall description of the experimental results and yielded reliable estimates of the equilibrium sorption parameters in aqueous solution. At pH 4.6, the monolayer sorption capacity (Q_m) of the copolymers with PNP varied from 0.359–2.20 mmol/g. At pH 10.3, the value of Q_m for the copolymers was significantly attenuated (0.070–0.191 mmol/g) due to electrostatic repulsions between the carboxylate anion sites of PAA and the anion form of PNP. The variable surface area results obtained from the solid-gas and solid-solution adsorption methods are attributed to hydration effects and swelling of the copolymer framework in solution relative to the solid state. CD-based copolymer materials with tunable physicochemical properties were prepared with variable comonomer content and efficient uptake of organic contaminants in aqueous solution. The copolymer materials have numerous potential applications for sorption-based processes, and further studies are underway to improve their molecular recognition properties for a variety of environmental conditions (i.e., pH, temperature, concentration). Some examples of potential applications involving copolymer materials containing β-CD and poly(acrylic acid) include the development of functional hydrogels as pharmaceutical excipients,[33] controllable nano-assemblies for materials design,[34] chemically responsive sol–gel materials,[35] biomimetic agents with tunable rheology,[36] and functional nano- to microscale coatings.[37]

References

1. Sun, Y.; Chen, J. L.; Li, A. M.; Liu, F. Q.; Zhang, Q. X. React Funct Polym 2005, 64, 63.
2. Yin, J.; Chen, R.; Ji, Y.; Zhao, C.; Zhao, G.; Zhang, H. Chem Eng J 2010, 157, 466.
3. Lanouette, K. H. Chem Eng 1977, 84, 99.
4. End Poverty 2015: Millennium development goals. United nations website. Available at: http://www.un.org/millenniumgoals/. (accessed August 23, 2011).
5. Inoue, Y.; Harkushi, T.; Liu, Y.; Tong, L. H.; Shen, B. J.; Jin, D. S. J Am Chem Soc 1993, 115, 475.
6. van de Manakker, F.; Vermonden, T.; van Nostrum, C. F.; Hennink, W. E. Biomacromolecules 2009, 10, 3157.
7. Jang, J. S.; Bae, J. Macromol Rapid Commun 2005, 26, 1320.
8. Park, H.; Robinson, J. R. Pharm Res 1987, 4, 457.
9. Bibby, D. C.; Davies, N. M.; Tucker, I. G. Int J Pharm 1999, 187, 243.
10. Bibby, D. C.; Davies, N. M.; Tucker, I. G. Int J Pharm 1999, 180, 161.
11. Emmett, P. H.; Brunauer, S. J Am Chem Soc 1937, 59, 1553.
12. Sing, K. S. W. Chem Ind 1967, 829.
13. Deboer, J. H.; Lippens, B. C.; Linsen, B. G.; Broekhof, J. C.; Vandenhe, A.; Osinga, T. J. J Coll Interface Sci 1966, 21, 405.
14. Barrett, E. P.; Joyner, L. G.; Halenda, P. P. J Am Chem Soc 1951, 73, 373.
15. Huglin, M. B.; Liu, Y.; Velada, J. L. Polymer 1997, 38, 5785.
16. Mohamed, M. H.; Wilson, L. D.; Headley, J. V.; Peru, K. M. IChemE: Proc Saf Env Prot 2008, 86, 237.
17. Dupuy, G.; Hilaire, G.; Aubry, C. Clin Chem 1987, 33, 524.
18. Giles, C. H.; D' Silva, A. P.; Tridevi, A. S. J Appl Chem 1970, 20.
19. Freundlich, H. M. Phys Chem A 1906, 57, 385.
20. Langmuir, I. J Am Chem Soc 1918, 40, 1361.
21. Brunauer, S.; Emmett, P. H.; Teller, E. I. J Am Chem Soc 1938, 60, 309.
22. Sips, R. J Am Chem Soc 1948, 125, 6452.
23. Pratt, D. Y.; Wilson, L. D.; Kozinski, J. A.; Morhart, A. M. J Appl Polym Sci 2010, 116, 2982.
24. Xu, W. L.; Liu, J. D.; Sun, Y. P. Chin Chem Lett 2003, 14, 767.
25. Sing, K. S. W.; Everett, D. H.; Haul, R. A. W.; Moscou, L.; Pierotti, R. A.; Rouquerol, J.; Siemieniewska, T. Pure Appl Chem 1985, 57, 603.
26. Yu, J. C.; Jiang, Z. T.; Liu, H. Y.; Yu, J. G.; Zhang, L. Z. Anal Chim Acta 2003, 477, 93.
27. Mohamed, M. H.; Wilson, L. D.; Headley, J. V. Carbohydr Res 2011, 346, 219.
28. Wilson, L. D.; Mohamed, M. H.; Headley, J. V. J Coll Interface Sci 2011, 357, 215.
29. Li, J.; Meng, X.; Hu, C.; Du, J. Biores Tech 2009, 100, 1168.
30. Kwon, J. H.; Wilson, L. D. J Environ Sci Health A 2010, 45, 1793.
31. BlancoFuente, H.; AnguianoIgea, S.; OteroEspinar, F. J.; BlancoMendez, J. Biomaterials 1996, 17, 1667.
32. Wilson, L. D.; Mohamed, M. H.; Berhaut, C. L. Materials 2011, 4, 1528; doi:10.3390/ma4091528.
33. Zhu, W.; Li, Y.; Liu, L.; Chen, Y.; Wang, C.; Xi, F. Biomacromolecules 2010, 11, 3086.
34. Yan, Q.; Xin, Y.; Zhou, R.; Yin, Y.; Yuan, J. Chem Commun 2011, 47, 9594.
35. Ogoshi, T.; Takashima, Y.; Yamaguchi, H.; Harada, A. J Am Chem Soc 2007, 129, 4878.
36. Hashidzume, A.; Tomatsu, I.; Harada, A. Polymer 2006, 47, 6011.
37. Lefort, M.; Popa, G.; Seyrek, E.; Szamocki, R.; Felix, O.; Hemmerlé, J.; Vidal, L.; Voegel, J.-C.; Boulmedais, F.; Decher, G.; Schaaf, P. Angew Chem Int Ed 2010, 49, 10110.